Regenerative Therapy 15 (2020) 226–235

Contents lists available at ScienceDirect

Regenerative Therapy

journal homepage: http://www.elsevier.com/locate/reth

Original Article

Proteomic analysis of platelet-rich and platelet-poor plasma

Olga Miroshnychenko [b, *, 2], Robert J. Chalkley [c], Ryan D. Leib [d], Peter A. Everts [e], Jason L. Dragoo [a, 1]

[a] Sports Medicine Center, 450 Broadway St., Pavilion C, Room C-433, MC 6120, Redwood City, CA, 94063, USA
[b] Department of Orthopaedic Surgery, Stanford University School of Medicine, 300 Pasteur Drive, Stanford, CA, 94305-5341, USA
[c] Mass Spectrometry Facility, University of California, San Francisco, 600 16th Street, Genentech Hall, suite N472A, San Francisco, CA, 94143-2240, USA
[d] Vincent Coates Foundation Mass Spectrometry Laboratory, Stanford University, 333 Campus Dr., Mudd Building, room 175, Stanford, CA 94305-4401, USA
[e] Gulf Coast Biologics. 4331 Veronica S. Shoemaker Blvd., Suite 2, Fort Myers, FL, 33916, USA

ARTICLE INFO

Article history:
Received 18 November 2019
Received in revised form
30 August 2020
Accepted 16 September 2020

Keywords:
PRP
PPP
Blood product
Pathway analysis
Growth factors
And cytokines

ABSTRACT

Background: Autologous blood products, such as platelet-rich plasma (PRP) are commercial products broadly used to accelerate healing of tissues after injuries. However, their content is not standardized and significantly varies in composition, which may lead to differences in clinical efficacy. Also, the underlying molecular mechanisms for therapeutic effects are not well understood.
Purpose: A proteomic study was performed to compare the composition of low leukocyte PRP, platelet poor plasma (PPP), and blood plasma. Pathway analysis of the proteomic data was performed to evaluate differences between plasma formulations at the molecular level. Low abundance regulatory proteins in plasma were identified and quantified as well as cellular pathways regulated by those proteins.
Methods: Quantitative proteomic analysis, using multiplexed isotopically labeled tags (TMT labeling) and label-free tandem mass spectrometry, was performed on plasma, low leukocyte PRP, and PPP. Plasma formulations were derived from two blood donors (one donor per experiment). Pathway analysis of the proteomic data identified the major differences between formulations.
Results: Nearly 600 proteins were detected in three types of blood plasma formulations in two experiments. Identified proteins showed more than 50% overlap between plasma formulations. Detected proteins represented more than 100 canonical pathways, as was identified by pathway analysis. The major pathways and regulatory molecules were linked to inflammation.
Conclusion: Three types of plasma formulations were compared in two proteomic experiments. The most represented pathways, such as Acute Phase Response, Coagulation, or System of the Complement, had many proteins in common in both experiments. In both experiments plasma sample sets had the same direction of biochemical pathway changes: up- or down-regulation. The most represented biochemical pathways are linked to inflammation.

1. Introduction

In the past two decades commercial formulations of platelet-rich plasma (PRP) have been increasingly used in orthopedic and other medical applications to augment the healing of soft tissue injuries or chronic inflammation [1–4]. PRP therapy is an appealing treatment due to its autologous nature, anti-microbial properties, and relatively easy preparation. Many authors have reported enhanced healing after PRP injection, but a lack of efficacy has also been widely reported [3–6].

The idea behind PRP usage is to increase the concentration of activated platelets at an area of damaged tissue, and thus achieve a

* Corresponding author.
E-mail addresses: olga_miro@pobox.com (O. Miroshnychenko), chalkley@cgl.ucsf.edu (R.J. Chalkley), rdleib@stanford.edu (R.D. Leib), peter@gulfcoastbiologics.com (P.A. Everts), j.dragoo@cuanschutz.edu (J.L. Dragoo).
Peer review under responsibility of the Japanese Society for Regenerative Medicine.
[1] Jason L. Dragoo, Professor and Vice Chairman, Endowed Chair of Regenerative Medicine, Head Team Physician Denver Nuggets, Team Physician Denver Broncos, Director, UC Health Steadman Hawkins Center. 175 Inverness Drive West, Suite 200, Englewood, CO 80112, USA. and (650) Fax: 303.694.9666.
[2] Olga Miroshnychenko, Adjunct Professor, Department of Biological Sciences, A301, New York City College of Technology, The City University of New York. 285 Jay Street, Brooklyn, NY 11201, USA.

https://doi.org/10.1016/j.reth.2020.09.004

List of abbreviations

C18	A resin for reversed-phase chromatography
DTT	Dithiothreitol, a reducing reagent also known as Cleland's reagent
ECM	Extracellular matrix
FT	Flow-through fractions in sample separation
IPA	Ingenuity Pathway Analysis software
LC-MS/MS	Liquid chromatography with tandem mass spectrometry
LTQ	Orbitrap Elite mass spectrometer, Thermo Scientific
ppm	Parts per million
PPP	Platelet-poor plasma
PRP	Platelet-rich plasma
RP	Reverse phase fractionation
SpeedVac	Vacuum concentrator
Swiss-Prot	Manually annotated, non-redundant protein sequence database, freely accessible
TEAB	Triethylammonium bicarbonate
TCEP	Reducing agent tris (2-carboxyethyl) phosphine
TMT	Tandem mass tags
UniProt	Database of protein sequence and functional information, freely accessible
UPLC	Ultra-performance liquid chromatography

many-fold increase of concentration of growth factors and cytokines released by platelets. While PRP treatment has never been reported as harmful, the clinical efficacy of the procedure remains variable, probably due to the varied composition and properties of PRP formulations [4,7–10]. Factors of variability include but are not limited to: 1) medical conditions and ages of patients, 2) manufacturers of PRP devices, 3) different protocols used for PRP preparation, 4) different content of cells, e.g. thrombocytes, leukocytes, and levels of cell-secreted regulatory molecules in PRP, because of the preceding. Proteomic analysis can address some of these differences in PRP composition, and potentially relate them to the specific steps of the protocols that are being used for their generation.

Several research groups observed negative biological effects in cell culture of too high numbers of platelets, as well as high numbers of lymphocytes in human blood plasma products [4,5,10–13]. For example, synoviocytes [14] and human ligament fibroblasts [5] treated with such PRP showed increased MMP secretion, and proinflammatory response [4,15].

Successful usage of leucocyte-rich PRP was also demonstrated in vitro and in vivo [16]. A number of clinical trials showed the effectiveness of leucocyte-rich PRP in treating orthopedic injuries such as gluteal tendinopathy, plantar fasciitis, tennis elbow, compared to alternative options [17–21]. Both leucocyte-rich and leucocyte-poor types of PRP are broadly used to treat musculoskeletal injuries.

According to Pifer et al. [5] "future studies are necessary to understand anabolic, catabolic, and inflammatory factors in PRP and how they affect various pathologic states in soft tissues." In agreement with this, Murray writes in an editorial that "optimal PRP formulations should be established for specific indications" [8]. Other authors have expressed similar views; it is possible that a range of certain cell types, as well as levels of regulatory proteins in PRP, have tissue-specific optima and need to be controlled. Such optimization could be critical in assisting healing of different tissue types, but the tissue-specific ranges remain to be established [3,8–10,13,22]. Enhanced concentration of certain regulatory molecules, e.g. growth factors and cytokines, released by cells could lead to suboptimal levels of inflammation, fibrotic, apoptotic, and catabolic processes [23,24].

Proteomic analysis is a suitable technology to assess the protein content of plasma formulations during method development. Mass spectrometry-based proteomic methods are the most common technologies for the large-scale study of proteins and peptides on a picomole, or even femtomole level [25,26].

The aim of this paper is to quantify and characterize the protein composition in 1) leukocyte poor PRP and in 2) platelet poor plasma (PPP). As a pilot study, we evaluated only plasma formulations derived from two blood donors; the next phase of investigation would include several donors of blood plasma, up to ten, which would be processed into PRP and PPP for further proteomic analysis. This would allow applying biostatistical analysis to mass-spectral results. Proteomic data were further analyzed using Ingenuity Pathway Analysis (IPA) and the DAVID resources, which allowed the comparison of plasma formulations on molecular and pathway levels [27,39].

2. Materials and Methods

2.1. Blood processing: preparation of PRP and other plasma fractions

After Institutional Review Board approval[3], two healthy donors provided 50 mL of blood, which was processed to produce leukocyte-poor plasma formulations. Blood was drawn in a clinical laboratory.

Blood was processed using Pure PRP kit and a matching centrifuge from EmCyte Corp., with sodium citrate as anticoagulant [7,10]. Two plasma formulations were prepared: 1) traditional platelet-rich plasma, PRP, and 2) platelet poor plasma, PPP, according to the EmCyte manual for Pure PRP kit. Platelet enrichment or removal was controlled by an automatic complete blood count (CBC), which was performed for each blood donor for blood plasma, PRP and PPP using 1 mL of each fraction at Stanford Clinical Laboratory. White blood cells and platelets numbers are presented for each plasma fraction for donors in Table 1.

Aliquots of these fractions were immediately prepared for proteomic analysis, 10 mcl each. These aliquots were flash-frozen in liquid nitrogen after addition of protease inhibitor cocktail (#78429, Thermo Fisher Scientific) and stored at −80 °C.

2.2. Sample preparation for mass-spectrometry

Plasma fractions from two human donors were analyzed by mass spectrometry, using the experimental protocols described below. Please see Fig. 1 for the Scheme of procedures.

2.3. Multiple Affinity Removal System, MARS

MARS system (# 5188–6560 and #5188–5254, Agilent) was used for immunodepletion of 14 high-abundance proteins in 10 mcl aliquots of all plasma samples: albumin, IgG, antitrypsin, IgA, transferrin, haptoglobin, fibrinogen, alpha 2-macroglobulin, alpha1-acid glycoprotein, IgM, apolipoprotein AI, apolipoprotein AII, complement C3, and transthyretin. Processing of ten microliters of each plasma formulation resulted in one ml of flow-through (FT)

[3] The study's protocol was approved by institutional review board (IRB). Research Compliance Office, Stanford University, 3000 El Camino Real; Five Palo Alto Square, Palo Alto, CA 94306.

sample, a depleted plasma sample, containing medium- and low-abundance proteins (~5% of initial protein amount). These depleted (FT) samples were concentrated using a 3MWCO Amicon centrifugal filter unit (UFC500324, EMD Millipore) to 25 mcl, and the buffer was replaced with 50 mM NH_4HCO_3. After depletion from high-abundance proteins, medium- and low-abundance proteins of plasma samples were digested in solution with an enzyme mixture of trypsin and LysC (details are in the paragraphs for Experiments I, and II), followed by LC-MS/MS analysis.

2.4. Experiment I. Preparation of three plasma samples for label-free MS analysis

Plasma, PRP, and PPP, 10 mcl of each, were depleted of abundant proteins (Fig. 1). Flow through (FT) fractions were concentrated, and after buffer exchange to 50 mM NH_4HCO_3, reduced and alkylated, followed by trypsin digestion. For reduction and alkylation, 20 μL of ProteaseMax solution, which is a surfactant to solubilize proteins (Promega, V2072), was added to 25 μL of depleted plasma samples in 50 mM NH_4HCO_3. Then to reduce disulfide bonds in proteins, 1.6 μL of 500 mM DTT stock was added to each sample, followed by incubation at 55 °C for 30 min. For alkylation of the resulting thiol groups, 3.2 μL of 1 M acrylamide was added to each sample, followed by incubation at room temperature for 30 min. After that, for proteolytic digestion Trypsin/Lys-C mix was added at a 1:50 ratio (Promega V5071, Trypsin/Lys-C Mix, Mass Spec Grade) on ice, and samples were incubated at 37 °C overnight. Tryptic digest was quenched by adding 5 μL of 50% formic acid in water. Samples were spun at 10,000 g for 10 min and desalted in a Stage Tip purification step. For sample desalting of label-free peptides we used reversed phase MicroSpin Columns, TARGA C18 SEM SS18R from NEST according to the operating instructions. Samples were concentrated in a vacuum centrifuge (SpeedVac Concentrator Savant from Thermo Scientific) and submitted to tandem mass spectrometry (LC-MS/MS).

2.5. Experiment I. Mass spectrometry data acquisition and database searches

Samples were analyzed by LC-MS/MS using a Nanoacquity UPLC system (Waters, Milford, MA) interfaced to a LTQ-Orbitrap Elite mass spectrometer (Thermo Scientific, San Jose, CA). Chromatography was performed using an Easy-Spray 75 um × 150 mm C18 column (Thermo Fisher, ES800) at a flow rate of 400 nl/min. The 60 min gradient ran from 2 to 25% of buffer B in 39 min, then to 70% B in a further 5 min, before returning to 2% B in 1 min to equilibrate for the next run. Buffer A was 0.1% formic acid; buffer B was acetonitrile in 0.1% formic acid. Survey scans were performed from m/z 350–1500, with ions measured in the Orbitrap at a resolution setting of 60 K. The top six multiply charged ions were selected for fragmentation analysis by resonant excitation collision-induced dissociation and measured in an ion trap. Precursors were then dynamically excluded from re-selection for 30 s. Raw data were analyzed using Protein Prospector v5.19.23 (PMID: 18653769). Searches were performed against the human entries in a Swiss-Prot database downloaded on May 9th, 2016, with concatenated randomized sequences (20,200 entries searched) to allow estimation of the false discovery rate [28]. Peptides were assumed to be fully tryptic. Precursor ion tolerance was set at ± 10 ppm and fragment tolerance was set at ± 0.6 Da. Propionamide modification of cysteines was considered as a constant modification; variable modifications considered were methionine and tryptophan oxidation, deamidation of asparagines, pyro-glutamate formation from peptide N-terminal glutamines, protein N-terminal methionine removal, acetylation, and combinations thereof. Results for each sample were reported at the 1–2% false discovery rate at the protein level. Quantitation was performed using spectral counting. **Pathway analysis** of protein lists for this data set was performed using Ingenuity Pathway Analysis database, IPA (39).

2.6. Experiment II. Protein quantitation using multiplexed isotopically labeled tags (tandem mass tags, TMT)

Plasma, PRP, and PPP plasma aliquots, 10 mcl of each, were depleted of abundant proteins (2.2 and 2.3). Protein concentration was measured with 660 nm Protein Assay Kit (Pierce, # 22,662). Reduction and alkylation were performed according to the manual for TMT 6-plex Isobaric Mass Tag Labeling Kit (Thermo Sci., # 90,061). Reducing agent TCEP (tris (2-carboxyethyl) phosphine) was dissolved at 200 mM in 100 mM triethylammonium bicarbonate (TEAB). Samples were incubated at 55 °C for 1 h with 5 mcl of 200 mM TCEP. For the reaction of alkylation 2.5 mcl of 750 mM iodoacetamide was added per sample. Incubation processed for 30 min at room temperature in vials protected from light, followed by adding 6x volume of cold acetone and precipitation overnight. Acetone-precipitated protein pellets were dissolved in 100 μL of 100 mM TEAB. For trypsin digestion in solution 20 μl ProteaseMax solution (Promega, V2072) was added to each sample. Trypsin/Lys-C mix, 0.5 mcg/1 mcl per sample, was then added at a 1:50 ratio (Promega V5071, Trypsin/Lys-C Mix, Mass Spec Grade) and incubated at 37 °C overnight. TMT 6-plex isobaric mass tag peptide labeling: TMT Label Reagents (with mass tags in the range 126–131 Da; Thermo Sci. # 90,061) were dissolved in 40 μL of anhydrous acetonitrile and added to each sample. The reaction proceeded for 1 h at room temperature and was quenched with 8 μL of 5% hydroxylamine followed by 15 min incubation. TMT labeled samples were combined into one sample in a new tube. The combined sample was desalted and fractionated off-line using high-pH Reversed-Phase Peptide Fractionation cartridge (Pierce, #84868) to produce eight peptide fractions, which were concentrated in a vacuum centrifuge, and submitted to tandem mass spectrometry.

2.7. Liquid chromatography mass spectrometry (LC-MS)

Each of the eight high-pH fractionated peptide pools was reconstituted in mobile phase A, and peptides loaded onto a self-packed C18 reversed phase column (C18, 2.4 μM, Dr. Maish, Germany) 35 cm in length. The UPLC was the ACQUITY UPLC M-Class System from Waters, where mobile phase A was 0.2% formic acid in water and mobile phase B was 0.2% formic acid in acetonitrile. For

Table 1
Platelet and white blood cell (WBC) count for donor samples used for proteomic study. All numbers represent cells x 10^3 per μl of blood fraction, except the row "Platelet enrichment in PRP" representing fold change compared to plasma.

Blood donor number	I	II
WBC in blood	4.4	4.5
WBC in plasma	0.8	0.9
WBC in PRP	0.6	0.3
Platelets in blood plasma	152	264
Platelets in PRP	685	472
Platelets in PPP	6	6
Platelet enrichment in fold change by PRP preparation	4.5	1.8

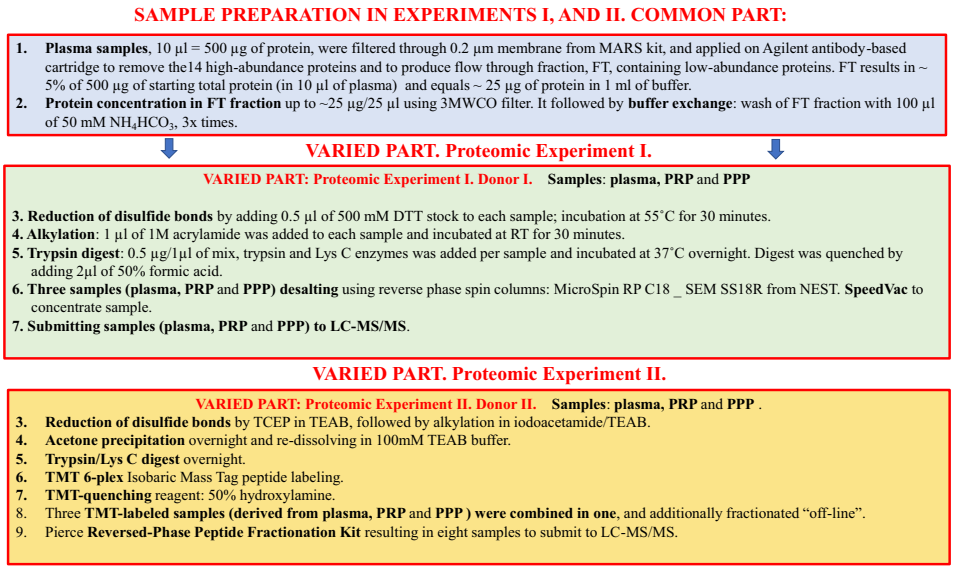

Fig. 1. Scheme of common procedures and differences between sample processing in two experiments. Details are in the text, subsections 2.3–2.8.

each fraction a 180 min separation gradient was used, where the starting mobile phase B percentage was 4% ramped up linearly to 42%, followed by a wash and re-equilibration step. The flow rate was 300 nl/min. The mass spectrometer was an Orbitrap Fusion, where peptides were ionized in positive mode at a spray voltage of 1800 V. The methodology used was a MS3 (synchronous precursor scan SPS) method where the isobaric peptides were fragmented first in the ion-trap followed by a "notch" event isolating (0.7Da) the 5 most intense fragment ions. These ions were then subsequently fragmented using HCD and transferred to the Orbitrap, where the scan range was set at 120–500 *m/z* with a resolution setting of 60,000. Charge states analyzed were 2+-6+ where the AGC settings for the two MSMS events were 50,000 and 100,000 ions, respectively. A dynamic exclusion list was used, based on precursor mass ± 10 ppm and an exclusion duration of 90 s. Formic acid, trifluoroacetic acid, acetonitrile, and water were of LC-MS grade from Pierce.

2.8. Peptide identification and isobaric reporter ion quantification

Raw files containing MS/MS spectra were qualified using Preview software (Protein Metrics, San Carlos, CA) to validate peptide observations and overall quality before proceeding to peptide assignment. Peptide assignment and protein inference were made using Byonic MS/MS search engine v2.6.49 (Protein Metrics, San Carlos, CA) as a node in Proteome Discoverer (Thermo Scientific, San Jose, CA), which was used to assign quantitative ratios for isobaric-tagged samples. Samples were searched against the Uniprot *Homo sapiens* protein database, containing isoforms (January 2016). Assignments were made to semi-tryptic peptides, with 12 ppm mass tolerances for precursor ions, 0.4 Da tolerances for fragment ions, and 12 ppm tolerances for MS3 reporter ion measurements. All data were validated using a standard 1% false discovery rate as introduced by Gygi and coworkers using a reverse-decoy technique [28]. The resulting mass spectral data, including peptide spectral matches and assigned proteins, were exported for visualization and statistical characterization. **Pathway analysis** of protein lists for this set of data was performed using both IPA and David databases (David db.) [27,39].

2.9. Pathway analysis software

Ingenuity Pathway Analysis (IPA, QIAGEN) software was used to analyze and interpret all sets of experimental data. Protein lists and mass-spectral peak counts in Experiment I, or ratios for TMT-labeled samples in Experiment II were used as input 39]. **David database**, version 6.7, was also applied for pathway analysis using gene list as an input in Experiment II (2.6–2.8) [27].

Venn diagrams were made using the software tool available at the URL in reference [40].

3. Results

3.1. Quantitative proteomic analysis of blood plasma, PRP, and PPP formulations

3.1.1. *Experiment I* (blood donor # 1)

About 320 proteins were detected in total in three types of samples: plasma, PRP, and PPP. For the complete list of proteins in these formulations, and their relative expression, presented as a heat map, see Supplemental Materials, Table I. About 50% of proteins were found in common in all three fractions (Fig. 2). In a comparison of fractions, about 130 proteins with various important functions, such as calcium-binding proteins SPARC (osteonectin) calmodulin and calumenin, enzymes catalase and superoxide dismutase, platelet glycoprotein V and platelet factor 4, type 1 collagen, talin and transforming growth factor beta-1, were detected in traditional PRP fraction, but not in PPP (Table 2, Fig. 2). Fifteen proteins were detected only in PPP fraction, but not in plasma, or PRP. This group included functionally important aminopeptidase N, hepatocyte growth factor-like protein, von Willebrand Factor and selenoprotein P (Table 2). Nine proteins were detected only in plasma sample (Fig. 2 and Supplementary Table I), List of proteins in plasma formulations, and a heat map of their relative expression).

About 50% of identified proteins were found in all three plasma fractions or shared between two plasma samples. It is infeasible to list and describe all of the quantitative and qualitative differences in the identified proteins amongst all plasma formulations (Supplementary Table I. List of proteins in plasma formulations, and a heat map of their relative expression). Therefore, we applied Ingenuity pathway analysis, IPA, which revealed more than a hundred biochemical pathways, with typically 20–40 proteins identified in each pathway per experimental group. Top canonical pathways and levels of their activation, based on IPA-generated heat map, are shown in Table 3 and Supplementary Table II (Full list of canonical pathways identified by IPA for the Experiment I, including proteins in each pathway for each blood plasma sample).

List of all pathways detected, including lists of proteins for each pathway, can be found in the Supplementary Table II. Heatmap for pathways detected in plasma fractions in Experiment I can be found in Supplementary Table III. Selected major pathways identified by IPA in plasma samples with their components are shown in Table 4.

3.1.2. *Experiment II* (blood donor # 2)

Samples of plasma, PRP and PPP in this proteomic experiment were TMT-labeled for quantification after a tryptic/Lys C enzymatic digest step, as described in Material and Methods. About 450 proteins were determined altogether in these three fractions by Byonic software (as described in Material and Methods). Results of mass spectral analysis were presented as a ratio between levels of proteins in PRP and PPP compared to protein levels in plasma. A full list of proteins for Experiment II and a heat map of individual protein levels' changes in plasma fractions can be found in Supplementary Table IV.

The DAVID database search engine recognized 20 proteins out of 450 proteins in this data set as being released by platelet alpha granules. Also, serine proteases (>20) and serpins, their inhibitors (>20) were detected. Several acute phase *pentaxin* proteins were identified: *serum amyloid P-component* and *C-reactive protein,* which was decreased in PPP compared to PRP and plasma (in this order). Another detected acute phase protein is *hemopexin*; its synthesis is induced after inflammation. Multiple components of the complement system were significantly enhanced in PRP and PPP compared to plasma sample. Among proteins that changed in level, several extracellular matrix-receptor interactors were identified.

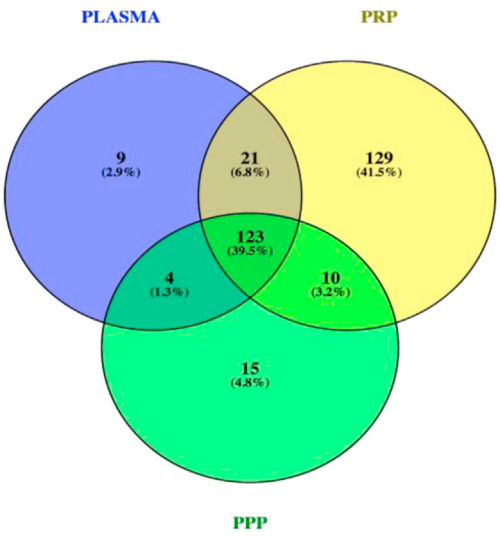

Fig. 2. Experiment I. Venn diagram comparison of three plasma fractions.

Individual protein changes in the plasma formulations can be seen in the Supplementary Table IV.

The following major pathways were identified using IPA and DAVID databases in all plasma fractions.

1) acute inflammatory response, represented by more than 20 proteins, according to both the IPA and DAVID databases; 2) wound healing, approximately 30 proteins per type of plasma; 3) complement activation, about 30 proteins per plasma sample; 4) leukocyte migration, about 10 proteins per sample; 5) cell structure and motility, about 30 proteins in each type of plasma, and many more processes, or canonical pathways. Both databases returned similar results in pathway detection, with a better overlap in major pathways.

A list of the top canonical pathways determined by IPA, and the major components of these pathways detected in Experiment II in all three plasma fractions can be seen in Table 4.

Several proteins were highly abundant in PPP compared to PRP: *fibronectin* (*FN),* a notable multifunctional glycoprotein of the extracellular matrix that binds to integrins, collagens, fibrin, proteoglycans, etc. *FN* is known for its involvement in acute phase reactions, cell motility, wound healing, fibril formation, and more [29]. Other abundant proteins were *fibulin*, *selenoprotein P*, *thrombospondin* (a multifunctional protein of blood platelet alpha-granules). Examples of proteins that were in low concentration in both, PRP and PPP, compared to plasma include *angiotensinogen*, *antithrombin III*, *catalase*, *platelet basic protein* and several other proteins (Supplementary Table IV. Full list of proteins for the Experiment II and a heat map of relative protein levels).

3.2. Regulatory proteins identified in plasma fractions by mass-spectrometry or predicted by IPA in proteomic experiments I and II

In both experiments we detected several growth factors and cytokines. These regulatory molecules are important for cell stimulating effects of PRP, and their relative levels in plasma formulations, are presented in Table 5.

The Comparison Analysis mode within the IPA program allows the prediction of the upstream regulators for individual pathways. Although most of these molecular regulators were not detected directly by mass-spectral analysis, due to their levels in plasma below the technical detection threshold, such prediction was possible based on quantitative changes of proteins in our data sets (Table 6).

The top regulator in both data sets was IL6, so we have provided an illustration only for its protein interactions (Fig. 3). In the Experiment II in IL6 pathway, apolipoprotein B, fibrinogen alpha chain and heat shock protein were more than two-fold up-regulated in PPP and PRP compared to plasma, while alpha-1-antichymotrypsin, angiotensinogen, and thrombospondin-1 were significantly down-regulated in PPP and PRP compared to plasma (Supplementary Table IV).

Other top predicted regulators that appeared similar in two proteomic experiments were HNF1 and HNF4 (transcriptional activators of the homeobox family), TGFbeta1, IL-1b, TNFa and SMAD3 (Table 6).

4. Discussion

Quantitative proteomics analysis facilitates in-depth analysis of biological systems. Such analysis of plasma content would aid in understanding effects of plasma formulations, controlling their production or targeted modification for therapeutic applications.

Here we present proteomic analysis of plasma formulations, including low leukocyte PRP and PPP, which exerted multi-fold biological effects on myoblast differentiation and proliferation

Table 2
Proteins detected by mass-spectral analysis only in one of the plasma fractions in Experiment I, which reflects differences in plasma formulations.

# of proteins in plasma fraction	Proteins detected by mass-spectrometry analysis in only one plasma fraction
Proteins detected only in **PRP** (129):	Vinculin; Alpha-enolase; Moesin; Radixin; Actin; alpha cardiac muscle 1; 14-3-3 proteins zeta/delta, beta/alpha and protein epsilon; Heat shock cognate 71 kDa protein and Heat shock 70 kDa protein 1 A; Alpha-actinin-1; Alpha-actinin-4; Zyxin; Peptidyl-prolyl cis–trans isomerase A; Cofilin-1; Profilin-1; Caldesmon; Adenylyl cyclase-associated protein 1; Hemoglobin subunits beta and delta; Pyruvate kinase PKM; Tropomyosin alpha-4 and beta chains; Glyceraldehyde-3-phosphate dehydrogenase Triosephosphate isomerase; Protein disulfide-isomerase A3; Calreticulin; Catalase; Protein deglycase DJ-1 Phosphoglycerate kinase 1; Carbonic anhydrase 2; Thrombospondin-1; Serum deprivation-response protein; Fructose-bisphosphate aldolase A; Pleckstrin; Rho GDP-dissociation inhibitor 2; Platelet glycoprotein V; Ras suppressor protein 1; Vasodilator-stimulated phosphoprotein; L-lactate dehydrogenase A chain; Rab GDP dissociation inhibitor alpha and beta; L-lactate dehydrogenase B chain; Coagulation factor V; Glucose-6-phosphate isomerase; Microtubule-associated protein RP/EB family member 2; Adenylate kinase isoenzyme 1; Peptidyl-prolyl cis–trans isomerase FKBP1A; PDZ and LIM domain protein 1; Calmodulin; Alpha-endosulfine; Ras-related protein Rap-1b; Fermitin family homolog 3; SH3 domain-binding glutamic acid-rich-like protein 3; Annexin A5; Phosphoglycerate mutase 1; Rho GTPase-activating protein 1; Nucleosome assembly protein 1-like 1; Protein disulfide-isomerase A6; Peroxiredoxin-6; Glutathione S-transferase P; Eukaryotic translation initiation factor 4H; Ras-related protein Rab-7a; WAS/WASL-interacting protein family member 1; Serglycin; Purine nucleoside phosphorylase; SH3 domain-binding glutamic acid-rich-like protein; Chloride intracellular channel protein 1; Reticulon-4; Phosphoglucomutase-1; Thymidine phosphorylase; Phosphatidylethanolamine-binding protein 1; Flavin reductase (NADPH); Plasminogen activator inhibitor 1; Talin-1; Peroxiredoxin-1 and -2; Rho GDP-dissociation inhibitor 1; Nidogen-1; Trans-Golgi network integral membrane protein 2; Coactosin-like protein; Polymeric immunoglobulin receptor; Src substrate cortactin; D-tyrosyl-tRNA (Tyr) deacylase 1; Prothymosin alpha; Beta-parvin; Neurogranin; Ig kappa chain V-III region SIE; Ig gamma-2 chain C region; Phosphatidylcholine-sterol acyltransferase; Small ubiquitin-related modifier 3; SPARC (Osteonectin); Microtubule-associated protein RP/EB family member 1; Integrin alpha-IIb; Collagen alpha-1(I) chain; Heparanase; Transforming growth factor beta-1; Malate dehydrogenase, cytoplasmic; Adenine phosphoribosyltransferase; Peptidyl-prolyl cis–trans isomerase FKBP3; Actin-related protein 2/3 complex subunit 1 B; Calumenin; Cysteine and glycine-rich protein 1; SH3 domain-binding glutamic acid-rich-like protein 2; Septic-7; Peptidyl-prolyl cis–trans isomerase NIMA-interacting 1; Superoxide dismutase [Cu–Zn]; Basement membrane-specific heparan sulfate proteoglycan core protein; Intraflagellar transport protein 140 homolog; S-arrestin; Serine/threonine-protein phosphatase 2 A activator;; Ubiquitin-conjugating enzyme E2 variant 1; Platelet factor 4; Target of Nash-SH3; Endonuclease domain-containing 1 protein; Protein CDV3 homolog; Cyclin-dependent kinase 2-associated protein 1; Ubiquitin-conjugating enzyme E2 N; Receptor-type tyrosine-protein phosphatase; Dynein heavy chain 1, axonemal; Ig alpha-1 chain C region; Tight junction protein ZO-2; Amyloid beta A4 protein
Proteins detected only in **PPP (15)**:	Aminopeptidase N; Proteoglycan 4; Selenoprotein P; Intercellular adhesion molecule 2; Ectonucleotide pyrophosphatase/phosphodiesterase family member 2; Neogenin; Hepatocyte growth factor-like protein; Hornerin; von Willebrand factor; Desmoglein-2; Granzyme K; Apolipoprotein D; Lysosome-associated membrane glycoprotein 2; Lysozyme C; Zinc finger and BTB domain-containing protein 46
Proteins detected only in **plasma** (9):	Transforming growth factor-beta-induced protein ig-h3; Mimecan; Neuropilin-1; Insulin-like growth factor-binding protein 6; CD44 antigen; Ezrin; Grainyhead-like protein 1 homolog; THAP domain-containing protein 5; Mannosyl-oligosaccharide 1,2-alpha-mannosidase IC

in an earlier study, as well as on protein biomarker expression [7].

We used sets of samples from two donors in two different experiments: different in sample preparation procedure (Fig. 1) followed by data acquisition, and protein identification in two mass-spectrometry centers, which used different instruments and software (see Materials and Methods, subsections 2.2; 2.4–2.8). The enormous dynamic range of protein concentrations in biological fluids is an analytical challenge for detecting important low-abundance proteins, which is broadly addressed by the proteomic community [25,26,30]. Therefore, we used two independent workflows: sample processing before mass-spectral analysis using TMT labeling of peptides versus label-free peptide identification as well as instrumentation, and proteomic software.

In all, nearly 600 proteins were detected in plasma formulations in two proteomic experiments. Plasma, PRP and PPP fractions had approximately 50% overlap in protein identification (Fig. 2 and Table 2). It appears that more proteins were identified in PRP than in the original plasma, which is related to the technical specifics of the method of mass-spectrometry and problem of the protein dynamic range in blood plasma (more than 10 orders of magnitude; therefore high abundance proteins mask low abundance proteins) [25,26].

Table 3
Activation of top canonical pathways in plasma formulations, based on IPA data. Pathways are listed in the order (decreasing) of statistical significance.

	Canonical pathway	Plasma	PRP	PPP
1	Acute phase Response Signaling	High	Low	High
2	Complement System	High	Low	Medium/high
3	Coagulation System	Medium	Low	High
4	LXR/RXR Activation	Medium	Low	Medium/high
5	FXR/RXR Activation	Medium	Medium/Low	Medium/high
6	Actin Cytoskeleton Signaling	Low	Medium/high	Low
7	Production of Nitric Oxide and Oxygen Species in Macrophages	Low	Low	Medium
8	Clathrin-mediated Endocytosis Signaling	Low	Low	Low
9	Integrin signaling	Low	Medium/high	Low
10	Glycolysis and gluconeogenesis	Low	High	Low
11	IL-12 signaling and Production in Macrophages	Low	Low	Medium
12	RhoA signaling	Low	Medium	Low
13	Hematopoiesis from Pluripotent Stem Cell Signaling	Low	Medium	Low
14	Leukocyte Extravasation Signaling	Low	High	Low

Table 4
Top canonical pathways and their components identified by IPA in Experiment II in plasma fractions.

#	Canonical pathway	Gene Names
1	[a]Acute Phase Response Signaling	IL6ST,SERPING1,ITIH3,FN1,APOA2,AMBP,C9,CP,FGG,F2,SERPIND1,C4A/C4B,C1R,MBL2,F8,ITIH2,ITIH4, CFB,FGB,SERPINA1,LBP,AGT,TTR,HPX,C3,C4BPB,C1S,AHSG,VWF, SAA4,SERPINF2,C5,PLG,KLKB1,ALB,HP,APOA1,TF,ORM1,C4BPA,CRP,ORM2,HRG,FGA,A2M,C2,RBP4
2	[a]Complement System	SERPING1,MASP2,C9,C1QA,C1QC,C1QB,C8A,C4A/C4B,C1R,MBL2,C7,CFB,CFI,CFH,CD59,C3, C4BPB,C1S,MASP1,C5,C4BPA,C8B,C6,C8G,C2
3	[a]Coagulation System	KNG1,F12,PROC,F13A1,VWF,F7,F2,SERPINF2,FGG,SERPIND1,PLG,F10,KLKB1, SERPINC1,F9,F8,PROS1,SERPINA5,F5,SERPINA1,FGB,FGA,A2M,F13B
4	[a]LXR/RXR Activation	KNG1,APOE, APOA4,APOB, APOA2,APOC4,AMBP,C9,APOC2,C4A/C4B,PON1,HPR,LCAT, ITIH4,SERPINA1,LBP, AGT,TTR,HPX,APOM,C3,AHSG,SAA4,A1BG,SERPINF2,APOL1,ALB,APOA1,ORM1,TF, APOC1,ORM2,CD14,PLTP,FGA,CLU,RBP4,APOC3
5	FXR/RXR Activation	KNG1,APOE, APOB,APOA4,APOA2,APOC4,AMBP,C9,APOC2,C4A/C4B,PON1,HPR, LCAT, ITIH4,SERPINA1,AGT,TTR,HPX,APOM,C3,AHSG, FETUB,SAA4,A1BG,SERPINF2,APOL1,ALB, APOA1,ORM1,TF,APOC1,ORM2,PLTP,FGA,CLU,RBP4,APOC3
6	Actin Cytoskeleton Signaling	KNG1,FN1,PFN1,CFL1,ARPC1B,ACTB,RDX,TLN1,GSN,F2,ACTA2,CD14, ACTG2,LBP,VCL,ACTN4,TMSB10/TMSB4X,ACTC1,ACTA1,ACTN1,MSNs
7	Production of Nitric Oxide and Reactive Oxygen Species in Macrophages	APOE, APOM,APOA4,APOB, APOC4,APOA2,APOC2,SAA4,APOL1,PON1,ALB,APOA1,ORM1,APOC1,ORM2, SERPINA1,CLU,RBP4,APOC3
8	Clathrin-mediated Endocytosis Signaling	APOE, APOA4,APOB,LPA,ACTB, APOA2,APOC2,F2,PON1,ALB,APOA1, TF,ACTA2,SERPINA1,ACTG2,ACTC1,ACTA1,CLU,RBP4,APOC3
9	Integrin signaling	RAP1B,ITGA2B,PFN1,ARPC1B,ACTB,TLN1,GSN,WIPF1,ACTA2,ZYX,ACTG2,ACTN4, VCL,ACTC1,CTTN, ACTA1,VASP, ACTN1
10	Glycolysis and gluconeogenesis	PGK1,ENO1,GPI,PGK2,TPI1,PGAM1,PKM,ALDOA, GAPDH;,MDH1
11	IL-6 signaling	COL1A1,CD14,LBP,A2M,IL6ST,CRP,CD14
12	IL-12 Signaling and Production in Macrophages	APOE, APOM,APOA4,APOB, APOC4,APOA2,MST1,APOC2,SAA4,APOL1,PON1,ALB,APOA1,ORM1,APOC1, ORM2,SERPINA1,CLU,RBP4,APOC3
13	RhoA signaling	PFN1,ARPC1B,CFL1,ACTA2,ACTB, SEPT7,RDX,ACTG2,ACTC1,ARHGAP1,ACTA1,MSN
14	Leukocyte Extravasation Signaling	RAP1B,VCAM1,ACTB,RDX,MMP2,WIPF1,ACTA2,CDH5,ACTN4,VCL,ACTG2,ARHGAP1, ACTC1,CTTN, ACTN1,ACTA1,VASP,MSN

[a] These pathways were significantly enhanced in PPP compared to PRP. Heatmap for pathways detected in plasma fractions (that illustrate quantitative differences between pathways in plasma, PRP and PPP samples) can be found in Supplementary Table V.

We did not provide similar Venn diagram (as in Experiment I; 3.1.1.) for proteins identified in plasma fractions in Experiment II, as proteomic software presented results as quantitative ratios for each protein in those plasma fractions and original blood plasma (Supplementary Table IV). Although experiments I and II were different from each other (Fig. 1), more than 200 proteins were found in common in both experiments, which is a good reproducibility for proteomic results and a solid justification of MS data that were used for the pathway analysis. Furthermore, both experiments, I and II, delivered very similar results of IPA software analysis, and identified activation or reduction of same major biochemical pathways, and often the same proteins (Tables 3-6 and Supplementary Table II, III and V).

Multiple Affinity Removal System, MARS, was used for immunodepletion of 14 high-abundance so-called 'house-keeping proteins' in plasma samples which are listed in the Materials and Methods. While a few additional proteins that bind to these may also get depleted, as the same treatment was applied to all samples, we expect the same proteins to be depleted in each of them. Therefore it should not affect the comparison between samples [30]. Also, major pathways detected by IPA and David Database in plasma samples are represented by 20 or many more proteins, and

Table 5
Regulatory proteins: growth factors, chemokines and their receptors identified in plasma fractions in proteomic experiments I and II. Indices [1,2] refer to the number of experiment where protein was detected.

Growth factors or cytokines	Regulation (↓ down, or ↑up)	Biological effects of a factor (based on the annotation in the UniProt database)
1 [1]Complement C5	No significant change between fractions	Chemokine that stimulates the locomotion of polymorphonuclear leukocytes and directs their migration toward sites of inflammation
2 [1,2] Hepatocyte growth factor activator & hepatocyte growth factor-like protein	↑ in PPP	Hepatocyte growth factor receptor signaling pathway
3 [1,2] Insulin-like growth factor-binding protein complex	No significant change	Involved in protein–protein interactions that result in protein complexes, receptor-ligand binding or cell adhesion.
4 [2] Isoform 2 of Insulin-like growth factor II	No significant change	Growth-promoting activity; in vitro mitogen. Exhibits osteogenic properties by increasing osteoblast mitogenic activity
5 [1,2] Pigment epithelium-derived factor	↓ in PPP in Experiment I	Potent inhibitor of angiogenesis
6 [1,2] Platelet basic protein	↑ in PRP	CXCR chemokine receptor binding; positive regulation of cell migration
7 [1]Platelet factor 4	↑ in PRP	Chemotactic for neutrophils and monocytes. Inhibits endothelial cell proliferation
8 [1,2] TGF beta-induced protein	↓in PRP, and absent in PPP in Experiment I	Plays a role in cell adhesion and perhaps in cell–collagen interactions
9 [1,2] Transforming growth factor beta 1	↑ in PRP	Multifunctional cytokine that controls cell growth, proliferation, differentiation, and apoptosis

Table 6
List of top predicted upstream regulators in plasma fractions generated by IPA software in Experiments I and II.

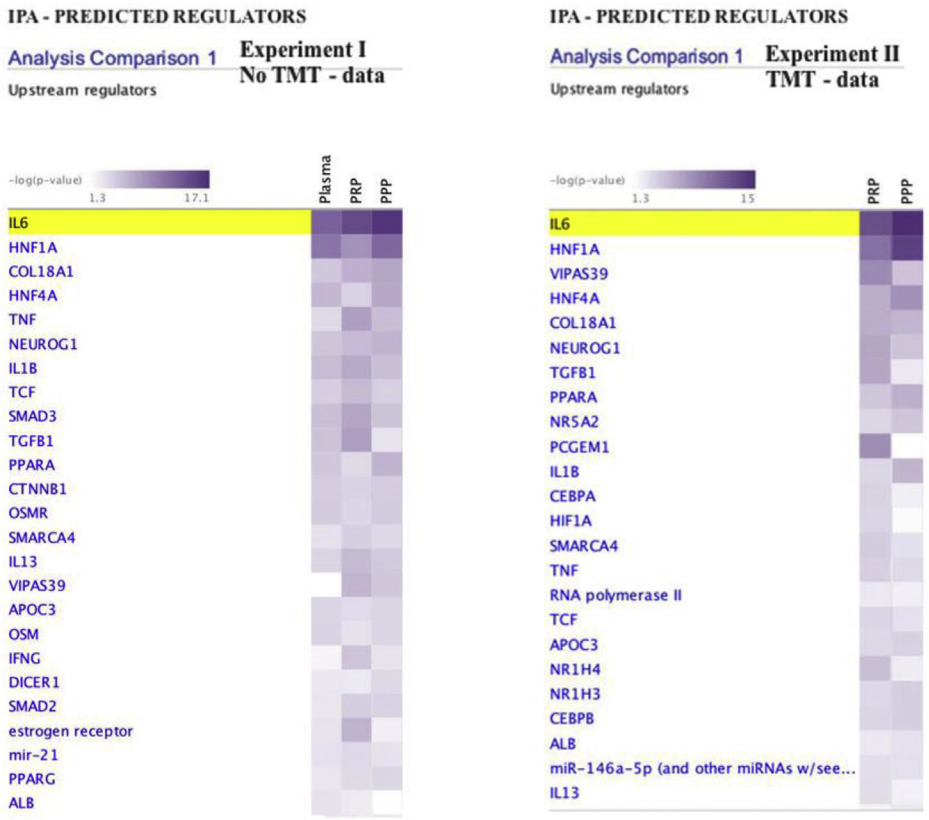

removal of one or two proteins from the pathway should not affect its detection and relative representation.

Platelet removal in PPP apparently eliminated or changed concentration of some regulatory proteins: pigment epithelium-derived factor, platelet basic protein, platelet factor 4, several Ca^{++} binding proteins, such as caldesmon, calmodulin, calreticulin and calumenin, multifunctional Heat shock protein Hsp 70 (Tables 2, 5 and Supplementary Table I and IV), as well as some yet unidentified factors, which lie below a technical threshold of mass-spectral detection. However, using IPA software, we were able to predict presence of such regulatory factors based on pathway analysis (Table 6). Differences in levels of these regulatory proteins, their presence, or absence, will affect numerous cell types and biological processes, like tissue healing, levels of inflammation, cell differentiation and proliferation [1,7]. However, establishing roles for individual factors that were present in changed concentration in PPP, compared to traditional PRP or plasma lies beyond the scope of this work; it would require a higher number of patient samples with laborious sample screening and validation.

We observed significant changes in canonical biochemical pathways between three plasma fractions. In both experiments, the major pathway, Acute Phase Response Signaling, was increased in PPP compared to PRP (Tables 3 and 4; Supplementary Table III and V). Acute Phase Response pathway is directly linked to inflammation; it is regulated by cytokines. This pathway includes plasma proteins, like C-reactive protein, serum amyloid A, transthyretin, fibronectin and others (Table 4 and Supplementary Table II), which change many-fold in response to injury [23,31,32]. A member of S100 protein family, hornerin, was enhanced in PPP formulation. It is known for its role in wound healing, and possible regulatory role in inflammatory immune response and proliferation [33].

Other top pathways detected by IPA: Coagulation, System of the Complement and LXR/RXR are also linked to inflammation through common pathway members [34–37]. These processes were also

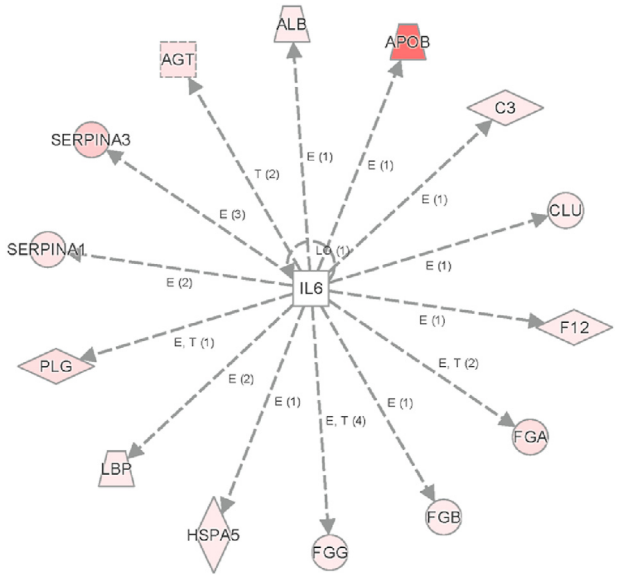

Fig. 3. IPA Comparison Analysis predicted IL6 as a top upstream regulator for protein expression changes in two proteomic data sets (for two different blood donors) [41].

activated in PPP compared to PRP in both experiments (Tables 3 and 4; Supplementary Table III and V).

The next regulatory pathways were only slightly activated in PPP compared to PRP: IL-12 Signaling and Production of Nitric Oxide (NO), while among the down-regulated pathways in PPP were: Clathrin-mediated Endocytosis Signaling, Actin Cytoskeleton Signaling and STAT3 pathway (Table 4, Supplementary Table II, III and V). Two other detected pathways, Wnt Signaling and PDGF Signaling, participate in switching cells between cell proliferation and differentiation [16,38]. However, we did not reliably trace changes for two last pathways due to the low level of their components. It is well established that both processes, differentiation and proliferation, are critical for tissue regeneration; cell switching between these processes is finely regulated and intersects with cell cycle pathways.

It was encouraging to see very close results in IPA analysis in both experiments despite individual variability between blood donors, and technical settings in mass spectrometry experiments. Repetitiveness of predicted regulatory molecules, many of which are known for pro-inflammatory properties: IL6, IL-1b, IL13, IFNG, TNFa, and more between two experiments was also encouraging (Table 6). Among predicted by IPA software upstream regulators for plasma fractions, IL6 was identified as the top regulator in both experiments (Table 6, Fig. 3). It is a potent inducer of the acute phase response, among a wide range of biological functions. IL6 affects B-cells, T-cells, hepatocytes, hematopoietic progenitor cells and cells of nervous system; it also acts as a myokine (22, 23).

Despite partial (~50%) overlap in protein identification between similar plasma fractions (reproducibility is an inherent limitation of the proteomic methods chosen), the major identified pathways and the directions of their changes were closely reproduced in two experiments.

5. Conclusion

This is a comparative biochemical proteomic study of platelet rich plasma, a commercial product for accelerated healing. In total, nearly 600 proteins were detected in plasma formulations in two proteomic experiments. They represented more than 100 canonical pathways, as was identified by IPA pathway analysis. The top pathways, such as Acute Phase Response, Coagulation, or System of the Complement, had many pathway members in common in both experiments. In both experiments plasma sample sets had predominantly same direction of biochemical pathway changes: activation or down-regulation.

Experiments I and II were different from each other in blood samples (donors I and II), in sample processing (TMT labeling of peptides in Experiment II), in instrumentation (different mass-spectrometers), and in proteomic data processing software. Nevertheless, more than 200 proteins were found in common in both experiments, which was a solid justification of proteomic results, which were used for the following pathway analysis. Main biochemical pathways detected by IPA in both experiments are linked to inflammation.

Conflict of Interest Statement

Peter A. Everts, PhD, FRSM, at the time of this study served as the Chief Scientific Officer of EmCyte Corporation. He contributed to manuscript writing support and detailed discussions, and did not participate in the execution of the study. Senior author Jason L. Dragoo, MD, received several disposable Pure PRP kits and a loan centrifuge for this study from EmCyte Corporation; no financial support was given. Olga Miroshnychenko, PhD, Robert J. Chalkley, PhD, and Ryan D. Leib, PhD, declare no conflict of interest.

[4] The node shapes, connecting lines, and marks are a graphic representation of Ingenuity Pathway Analysis.

Acknowledgments

We would like to thank the Department of Orthopaedic Surgery Stanford University School of Medicine, for the financial and material support provided to this study. Authors thank Dr. Chris Adams, who performed LC-MS/MS analysis for samples in Experiment II (2.6). We thank all our generous blood donors, whose names we cannot disclose here, for their dedication to medical research and providing their precious blood samples. Authors would like to thank Dr. Ewa Witkowska for reading the manuscript, her valuable comments, and suggestions. Our thanks to Kenneth J. Sheridan who carefully proofread the article.

Appendix A. Supplementary data

Supplementary data related to this article can be found at https://doi.org/10.1016/j.reth.2020.09.004.

References

[1] Textor J. Platelet-rich plasma (PRP) as a therapeutic agent: platelet biology, growth factors and a review of the literature. In: Lana JFSD, Andrade Santana MH, Dias Belangero W, Malheiros Luzo AC, editors. Platelet-Rich Plasma. Regenerative Medicine: Sports Medicine, Orthopedic, and Recovery of Musculoskeletal Injuries. 1 ed. Berlin Heidelberg: Springer-Verlag; 2014. p. 61–94.
[2] Hamid MS, Yusof A, Mohamed Ali MR. Platelet-rich plasma (PRP) for acute muscle injury: a systematic review. PLoS One 2014;9:e90538.
[3] Chellini F, Tani A, Zecchi-Orlandini S, Sassoli C. Influence of platelet-rich and platelet-poor plasma on endogenous mechanisms of skeletal muscle repair/regeneration. Int J Mol Sci 2019;20.
[4] DeLong JM, Russell RP, Mazzocca AD. Platelet-rich plasma: the PAW classification system. Arthroscopy 2012;28:998–1009.
[5] Pifer MA, Maerz T, Baker KC, Anderson K. Matrix metalloproteinase content and activity in low-platelet, low-leukocyte and high-platelet, high-leukocyte platelet rich plasma (PRP) and the biologic response to PRP by human ligament fibroblasts. Am J Sports Med 2014;42:1211–8.
[6] Giusti I, D'Ascenzo S, Manco A, Di Stefano G, Di Francesco M, Rughetti A, et al. Platelet concentration in platelet-rich plasma affects tenocyte behavior in vitro. BioMed Res Int 2014;2014:630870.
[7] Miroshnychenko O, Chang W-t, Dragoo JL. The use of platelet-rich and platelet-poor plasma to enhance differentiation of skeletal myoblasts. Implications for the use of autologous blood products for muscle regeneration. Am J Sports Med 2017;45:945–53.
[8] Murray IR, LaPrade RF. Platelet-rich plasma: renewed scientific understanding must guide appropriate use. Bone Joint Res 2016;5:92–4.
[9] Russell RP, Apostolakos J, Hirose T, Cote MP, Mazzocca AD. Variability of platelet-rich plasma preparations. Sports Med Arthrosc 2013;21:186–90.
[10] Wasterlain AS, Braun HJ, Dragoo JL. Contents and formulations of platelet-rich plasma. Operat Tech Orthop 2012;22:33–42.
[11] Graziani F, Ivanovski S, Cei S, Ducci F, Tonetti M, Gabriele M. The in vitro effect of different PRP concentrations on osteoblasts and fibroblasts. Clin Oral Implants Res 2006;17:212–9.
[12] Arnoczky SP, Shebani-Rad S. The basic science of platelet-rich plasma (PRP): what clinicians need to know. Sports Med Arthrosc Rev 2013;21:180–5.
[13] Sundman EA, Cole BJ, Fortier LA. Growth factor and catabolic cytokine concentrations are influenced by the cellular composition of platelet-rich plasma. Am J Sports Med 2011;39:2135–40.
[14] Browning SR, Weiser AM, Woolf N, Golish SR, SanGiovanni TP, Scuderi GJ, et al. Platelet-rich plasma increases matrix metalloproteinases in cultures of human synovial fibroblasts. J Bone Joint Surg Am 2012;94(23):e1721–7. https://doi.org/10.2106/JBJS.K.01501.
[15] Braun HJ, Kim HJ, Chu CR, Dragoo JL. The effect of platelet-rich plasma formulations and blood products on human synoviocytes: implications for intra-articular injury and therapy. Am J Sports Med 2014;42:1204–10.
[16] Li H, Usas A, Poddar M, Chen CW, Thompson S, Ahani B, et al. Platelet-rich plasma promotes the proliferation of human muscle derived progenitor cells and maintains their stemness. PLoS One 2013;8(6):e64923. https://doi.org/10.1371/journal.pone.0064923.
[17] Willits K, Kaniki N, Bryant D. The use of platelet-rich plasma in orthopedic injuries. Sports Med Arthrosc Rev 2013;21:225–30.

[18] Fitzpatrick J, Bulsara MK, O'Donnell J, Zheng MH. Leucocyte-rich platelet-rich plasma treatment of gluteus medius and minimus tendinopathy: a double-blind randomized controlled trial with 2-year follow-up. Am J Sports Med 2019;47:1130–7.
[19] Gosens T, Peerbooms JC, van Laar W, den Oudsten BL. Ongoing positive effect of platelet-rich plasma versus corticosteroid injection in lateral epicondylitis: a double-blind randomized controlled trial with 2-year follow-up. Am J Sports Med 2011;39:1200–8.
[20] Mishra AK, Skrepnik NV, Edwards SG, Jones GL, Sampson S, Vermillion DA, et al. Efficacy of platelet-rich plasma for chronic tennis elbow: a double-blind, prospective, multicenter, randomized controlled trial of 230 patients. Am J Sports Med 2014;42(2):463–71. https://doi.org/10.1177/0363546513494359.
[21] Peerbooms JC, Lodder P, den Oudsten BL, Doorgeest K, Schuller HM, Gosens T. Positive effect of platelet-rich plasma on pain in plantar fasciitis: a double-blind multicenter randomized controlled trial. Am J Sports Med 2019;47:3238–46.
[22] Maffulli N, Del Buono A. Platelet plasma rich products in musculoskeletal medicine: any evidence? Surgeon 2012;10:148–50.
[23] Scott A, Khan KM, Roberts CR, Cook JL, Duronio V. What do we mean by the term "inflammation"? A contemporary basic science update for sports medicine. Br J Sports Med 2004;38:372–80.
[24] Hudgens JL, Sugg KB, Grekin JA, Gumucio JP, Bedi A, Mendias CL. Platelet-rich plasma activates proinflammatory signaling pathways and induces oxidative stress in tendon fibroblasts. Am J Sports Med 2016;44:1931–40.
[25] Anderson NL, Anderson NG. The human plasma proteome: history, character, and diagnostic prospects. Mol Cell Proteomics 2002;1:845–67.
[26] Anderson NL, Polanski M, Pieper R, Gatlin T, Tirumalai RS, Conrads TP, et al. The human plasma proteome: a nonredundant list developed by combination of four separate sources. Mol Cell Proteomics 2004;3(4):311–26. https://doi.org/10.1074/mcp.M300127-MCP200.
[27] Dennis Jr G, Sherman BT, Hosack DA, Yang J, Gao W, Lane HC, et al. DAVID: database for annotation, visualization, and integrated discovery. Genome Biol 2003;4(5):P3.
[28] Elias JE, Gygi SP. Target-decoy search strategy for increased confidence in large-scale protein identifications by mass spectrometry. Nat Methods 2007;4:207–14.
[29] The UniProt C. UniProt: the universal protein knowledgebase. Nucleic Acids Res 2017;45:D158–69.
[30] Wu C, Duan J, Liu T, Smith RD, Qian WJ. Contributions of immunoaffinity chromatography to deep proteome profiling of human biofluids. J Chromatogr B Analyt Technol Biomed Life Sci 2016;1021:57–68.
[31] Ceciliani F, Giordano A, Spagnolo V. The systemic reaction during inflammation: the acute-phase proteins. Protein Pept Lett 2002;9:211–23.
[32] Gruys E, Toussaint MJ, Niewold TA, Koopmans SJ. Acute phase reaction and acute phase proteins. J Zhejiang Univ - Sci B 2005;6:1045–56.
[33] Gutknecht MF, Seaman ME, Ning B, Cornejo DA, Mugler E, Antkowiak PF, et al. Identification of the S100 fused-type protein hornerin as a regulator of tumor vascularity. Nat Commun 2017;8(1):552. https://doi.org/10.1038/s41467-017-00488-6.
[34] Wu Y. Contact pathway of coagulation and inflammation. Thromb J 2015;13:17.
[35] Tall AR, Yvan-Charvet L. Cholesterol, inflammation and innate immunity. Nat Rev Immunol 2015;15:104–16.
[36] Zelcer N, Tontonoz P. Liver X receptors as integrators of metabolic and inflammatory signaling. J Clin Invest 2006;116:607–14.
[37] Ricklin D, Lambris JD. Complement in immune and inflammatory disorders: pathophysiological mechanisms. J Immunol 2013;190:3831–8.
[38] Tanaka S, Terada K, Nohno T. Canonical Wnt signaling is involved in switching from cell proliferation to myogenic differentiation of mouse myoblast cells. J Mol Signal 2011;6:12.
[39] QIAGEN's Ingenuity® Pathway Analysis, IPA software, Redwood City, www.qiagen.com/ingenuity.
[40] Venn diagram was produced using URL: http://bioinfogp.cnb.csic.es/tools/venny/. Oliveros, J.C. (2007-2015) Venny. An interactive tool for comparing lists with Venn's diagrams. http://bioinfogp.cnb.csic.es/tools/venny/index.html..